INDIAN JOURNAL OF SCIENCE AND TECHNOLOGY

ORIGINAL ARTICLE

Check for updates

OPEN ACCESS

**Received:** 17/10/2024

**Accepted:** 16/04/2025

**Published:** 16/06/2025

**Citation:** Madhukumar R, Nayaka R, Mathad G, Subramanya K, Pathar D, Gurikar SG, Sali RK (2025) Influence of Ionizing Radiation on Bio-synthesis of Noble Metal SF-AgNPs: Their Applications. Indian Journal of Science and Technology 18(22): 1792-1800. https://doi.org/10.17485/IJST/v18i22.3428

* **Corresponding author**.

nwwton@gmail.com

**Funding:** None

**Competing Interests:** None

**Copyright:** © 2025 Madhukumar et al. This is an open access article distributed under the terms of the Creative Commons Attribution License, which permits unrestricted use, distribution, and reproduction in any medium, provided the original author and source are credited.

Published By Indian Society for Education and Environment (iSee)

**ISSN**
Print: 0974-6846
Electronic: 0974-5645

# Influence of Ionizing Radiation on Bio-synthesis of Noble Metal SF-AgNPs: Their Applications

**R Madhukumar[1]*, Ravikumara Nayaka[2], Gavisiddayya Mathad[3], K Subramanya[4], Deepa Pathar[3], Shivaraj G Gurikar[5], Raghavendra K Sali[6]**

**1** Assistant Professor, Department of Physics, R.T.E.S Degree College Ranebennur-581115, Karnataka, India
**2** Associate Professor, Department of Physics, G F G College Ranebennur- 581115,Karnataka, India
**3** Research Scholar , Department of Physics, Kuvempu University, Shankaraghatta Shivamogga-577451, Karnataka, India
**4** Assistant Professor, Department of Physics Sahyadri Science College, Kuvempu University, Shivamogga-577203, Karnataka, India
**5** Associate Professor, Department of Physics, SKNG GFG College, Gangavathi- 583227, Karnataka, India
**6** Assistant Professor, Department of Physics, J.S.S Arts, Science and Commerce College, Gokak-591307, Karnataka, India

## Abstract

**Objectives:** The aim of this study was to explore the rapid and extracellular synthesis of silver nanoparticles (AgNPs) using aqueous Bombyx Mori Silk fibroin (SF) solution, facilitated by UV irradiation. The study seeks to assess the stability, size, shape, and other key properties of the synthesized silver nanoparticles. **Methods:** Silver nanoparticles were synthesized by exposing the silk fibroin solution to UV radiation characterization of the synthesized AgNPs was carried out using various techniques, including UV-Vis spectroscopy to confirm nanoparticle formation, X-ray diffraction (XRD) for structural analysis, transmission electron microscopy (TEM) for morphological observation, Fourier transform infrared spectroscopy (FT-IR) to identify protein functional groups, and thermo gravimetric analysis (TGA) and differential scanning calorimetry (DSC) to assess thermal stability. **Findings:** UV-Vis spectra confirmed the formation of silver nanoparticles, with an increase in absorption corresponding to longer irradiation times. XRD analysis revealed a face centered cubic structure, indicating metallic silver nanoparticles. TEM images showed the nanoparticles to be spherical or nearly spherical in shape. FT-IR spectra indicated the involvement of silk fibroin proteins in the synthesis process. The TGA and DSC results demonstrated enhanced stability of the SF/AgNPs composites compared to bulk materials. **Novelty:** This study presents a simple, eco-friendly biosynthesis approach for silver nanoparticles using Bombyx mori silk fibroin and UV irradiation. The method provides a controlled synthesis process, allowing for the adjustment of particle size and shape through irradiation parameters, offering an alternative to more traditional physical and chemical methods in

nanoparticle synthesis. The stability and minimal chemical reactivity of the synthesized nanoparticles enhance their potential applications in various fields, including medicine, environmental protection, and nanotechnology.
**Keywords:** Bombyx mori silk; Silver nanoparticles; UV-Vis; TEM; TGA; DSC

# 1 Introduction

Nanoparticles (NPs) can be synthesized using various techniques, including physical, chemical, and biological approaches. Conventional methods, such as chemical and physical synthesis, have been widely employed for the production of silver nanoparticles (AgNPs). In recent years, metal nanoparticles—including gold, silver, palladium, and copper—have gained significant interest due to their unique properties and promising applications in thin film coatings[1], catalysis[2], chemical sensors[3], drug delivery[4], electronics[5], photochemistry, and photonics[6].Different synthesis methods provide alternative ways to control key parameters such as shape, size, surface functionalization, and interparticle distance, all of which influence the final properties of the nanoparticles. However, achieving precise control over these parameters remains a challenge, leading to extensive research in the field. Among these approaches, green synthesis has garnered attention, particularly the use of polymers as stabilizing and reducing agents. Despite their advantages, some of these methods involve reagents that may be harmful to the environment. To mitigate these effects, biological synthesis has emerged as a safer and more eco-friendly alternative, offering reduced toxicity and lower production costs. Biological synthesis of AgNPs can be achieved using precursors such as algae, microorganisms, lichens, and plant-based products.

Various techniques, including physical, photochemical, and biological methods, have been reported for AgNPs synthesis, each with its own advantages and limitations. Challenges such as scalability, cost, particle size distribution, and uniformity remain key considerations. Among physical methods, evaporation-condensation is commonly performed using a tube heating system under controlled pressure. The irradiation technique has also been explored for producing fine AgNPs.

Photochemical synthesis can be categorized into two main approaches: photophysical (top-down) and photochemical (bottom-up). In these methods, AgNPs are formed either through direct photoreduction of metal precursors or via the reduction of metal ions using photochemically generated excited species—a process known as photosensitization. One common photochemical method involves the use of silver nitrate ($AgNO_3$) along with an aqueous silk solution as a reducing agent.

Due to their broad applications, AgNPs are extensively used as antibacterial agents in various sectors, including healthcare, food storage, textile coatings, and industrial applications[7]. Their multi functionality and effectiveness make them highly valuable in numerous ecological and biomedical applications.

**Table 1.** Comparative analysis of AgNPs synthesis Methods

| Synthesis Method | Advantages | Limitations |
|---|---|---|
| Physical (e.g., evaporation-condensation, laser ablation) | Produces high-purity nanoparticles, avoids chemical contamination | Requires high energy, expensive equipment, limited control over size distribution |
| Chemical (e.g., reduction with chemical agents like sodium borohydride, citrate, silk solution) | Simple, scalable, allows controlled synthesis | Involves toxic reagents, potential environmental hazards |
| Photochemical (e.g., UV-induced reduction of AgNO3 with silk solution) | Environmentally friendly, avoids harsh chemicals, allows controlled growth | Requires optimization of light intensity and exposure time, limited scalability |
| Biological (e.g., using plant extracts, microorganisms, algae, enzymes) | Low toxicity, cost-effective, renewable sources | Difficulty in controlling size and morphology, batch-to-batch variations, stability issues |

# 2 Methodology

## 2.1 Preparation of silk fibroin (SF) solution

CSR2 cocoons were cut into small pieces and then treated twice with boiling aqueous solution of 0.02M $Na_2CO_3$, for 45 min to remove gumming material like sericin protein and rinsed with doubled distilled water to remove salts and other impurities and allowed to dry in air at room temperature. The degummed silk was dissolved in 9.3M LiBr salt solution at 60°C for 4h, then the obtained solution by this procedure is contaminated by Li ions, where it enters into the crystal domain of silk fibroin during the treatment. In order to remove the ions, silk fibroin solution is dialyzed by de-ionized water for 72h by changing the water for

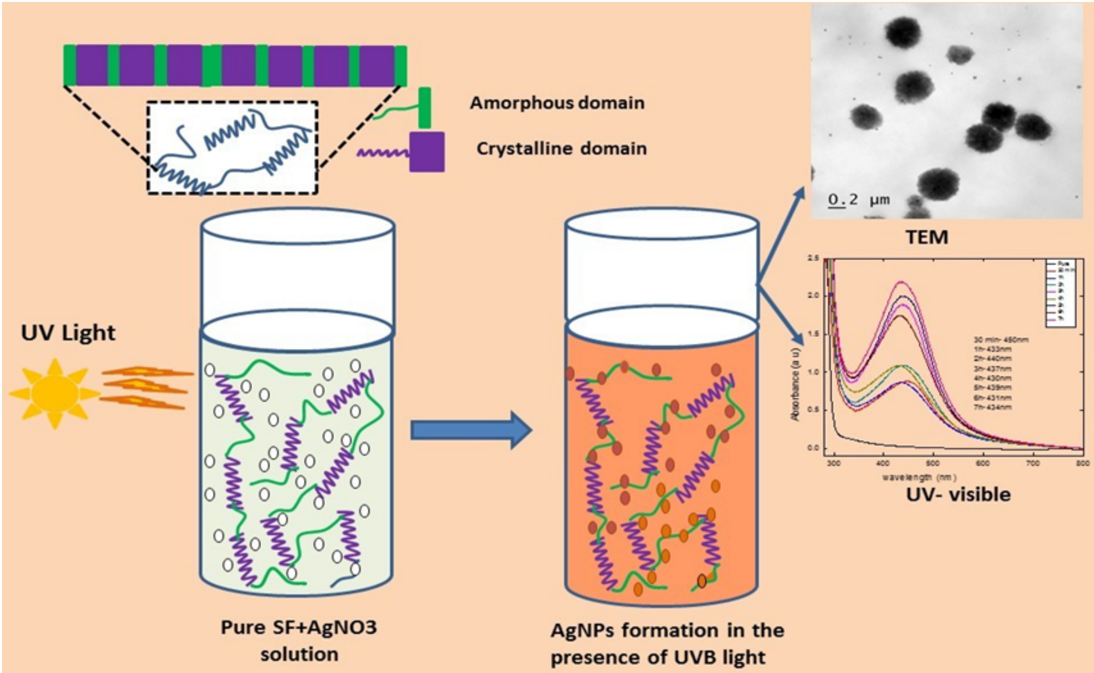


**Fig 1.** Synthesis of silver nanoparticles under UVB light irradiation

every 8 hours at room temperature using a dialysis Cassette (MWCO: 3500). Finally, the obtained optically clear solution was centrifuged at 4000r/min for about 20 min to remove small amount of undissolved silk aggregates formed during the process. Then, the clear solution of SF was stored at 4°C for further use. The concentration of SF was about 5wt% and was diluted to 1 wt.% by adding deionized water.

## 2.2 Preparation of SF-AgNPs solution

Ten to hundred milligrams of silver nitrate ($AgNO_3$) were added into 10mL of SF solution to form a transparent SF-$AgNO_3$ mixture solution. The final $AgNO_3$ concentration in the mixture was 10 mg/mL and then the SF-$AgNO_3$ mixture solution was subjected under the UVB light of intensity watt produce heat from light. The SF-$AgNO_3$ suspension were irradiated upto 4 hours the solution turns into golden yellow color, i.e. formation of SF-AgNPs composite solution. The prepared composite solutions were characterized at ambient temperature. The synthesized silver nanoparticles were confirmed by UV-Vis, XRD, TEM, SEM, EDAX, FTIR, TGA, and DSC.

## 2.3 Preparation of SF-AgNPs solution

Ten to hundred milligrams of silver nitrate ($AgNO_3$) were added into 10mL of SF solution to form a transparent SF-$AgNO_3$ mixture solution. The final $AgNO_3$ concentration in the mixture was 10 mg/mL and then the SF-$AgNO_3$ mixture solution was subjected under the UVB light of intensity watt produce heat from light. The SF-$AgNO_3$ suspension were irradiated upto 4 hours the solution turns into golden yellow color, i.e., formation of SF-AgNPs composite solution. The prepared composite solutions were characterized at ambient temperature. The synthesized silver nanoparticles were confirmed by UV-Vis, XRD, TEM, SEM, EDAX, FTIR, TGA, and DSC.

## 2.4 UV-Vis spectroscopy

UV-Visible (UV-Vis) spectra were measured using a spectrophotometer (Shimadzu UV-1800) in the wavelength range 190-800nm.

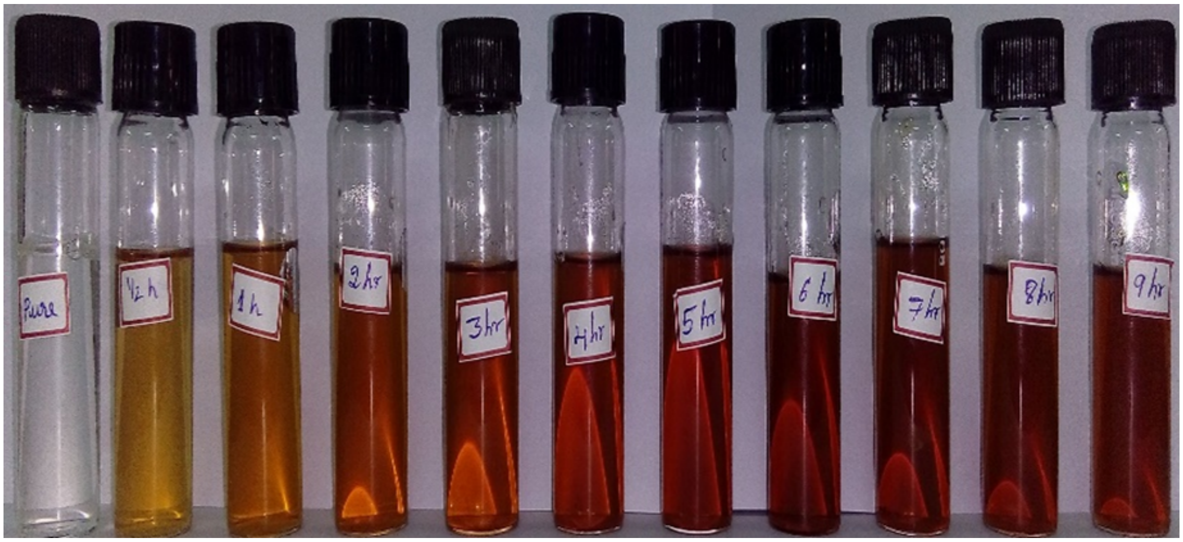


**Fig 2.** Silver nanoparticles solutions at different irradiation hours

### 2.5 Fourier transforms infrared spectra (FT-IR)

The FT-IR scans were used to identify the potential biomolecules in SF, which is responsible for reducing $Ag^+$ to $Ag^0$ FT-IR spectra of the SF and SF-AgNPs were measured by Perkin Elmer 2674 spectrometer having a resolution 4 $cm^{-1}$ in the wavenumber range 500-4000$cm^{-1}$.

### 2.6 Transmission electron microscopy (TEM)

The morphology of the silver nanoparticles was studied using transmission electron microscope (TEM), which was performed at 200kev using JEOL JEM2010. The selected area electron diffraction (SADE) data were also recorded.

### 2.7 Thermogravimetric analysis (TGA)

The degradation of silver nanoparticles was studied Thermogravimetric Analysis (TGA) was carried out with a TA instrument SDT Q 600. The samples were heated from room temperature to 600°C atheating rate of 10°C $min^{-1}$under a flow rate of nitrogen gas of 100ml/min.

### 2.8 Differential Scanning Calorimetry (DSC)

The thermal phase behavior of the samples was investigated by the Differential Scanning Calorimetry (DSC). Each sample was heated from room temperature to 600°C by heating rate 10°/min under a flow rate of nitrogen gas of 100ml/ min.

## 3 Results and Discussion

### 3.1 UV-visible Analysis

The absorption curves of pure SF and Ag/SF nanoparticles are shown in Figure 3.There is absorption band at about 275 nm of SF solution (which not visible) on the spectrum is mainly due to the $\pi$ to $\pi$*electron transition of the tyrosine (Tyr), phenylalanine (Phe) and tryptophan (Try) residue in SF chain. The pH value changes between 6-10 and shows a linear relationship with the concentration of SF at this peak. The average molecular weight of the amino acid residues is about 78, according to the composition of the amino acids in SF[8]. Thus the molar concentration of SF solution can be calculated from weight concentration at about around 450 nm, which are typical Plasmon resonance absorption attributed to colloidal silver particles[9]. The optical spectrum of the metal nanoparticles is dominated by the SPR which exhibits a shifting of wavelength depending upon the particle size, shape, and dispersions of the colloidal particles. Silk fibroin can reduce $Ag^+$ to $Ag^0$ by the strong electron donating property of its tyrosine (Tyr) amino acid residue. Meanwhile, UVB light irradiation is an effective method to assist the synthesis of AgNPs or Ag clusters on aqueous silk solution [10].

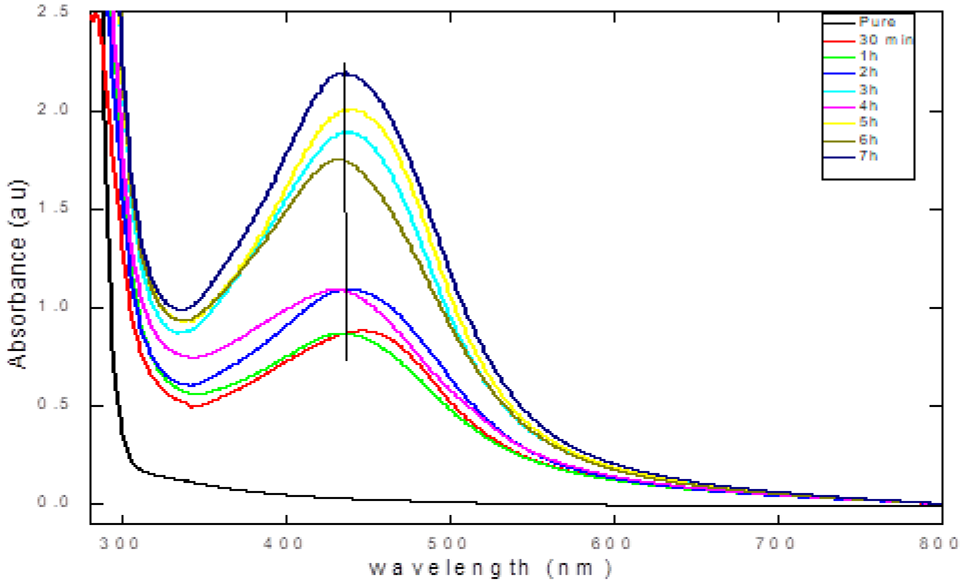


**Fig 3.** UV spectra of pure SF and SF/AgNPs

The absorption band in the visible light region is typical for Ag nanoparticles. In this study, AgNPs were synthesized from $Ag^+$ in aqueous SF solution under UVB light irradiation. The reduction $Ag^+$ ions into elemental Ag (i.e. AgNPs) in the aqueous solution was confirmed by color transition of the solution from yellow to brown color and is associated with an increase in the absorbance. AgNPs for which, maximum SPR intensity and wavelength represents a broad absorption band, with SPR at around 440nm-430nm indicate that nanoparticles are monodisperse system and they are in spherical in shape. The broader absorption band is an indication of larger particle size. From the absorption spectrum, the broadening of the peak increases with increasing the irradiation hours. On increasing the irradiation hours, the absorption peak gradually increases and shifts toward longer wavelengths. This is characteristic of increase in the irradiation time and size of silver nanoparticles. The amount of silver reduced, and the extent of silver agglomeration increase with the irradiation time. The particle size distributions have been studied by analyzing the TEM of nanoparticles having SPR maximum and minimum wavelengths as shown in Figure 4.

## 3.2 TEM Analysis

The morphology of the AgNPs in aqueous solution was confirmed using TEM as shown in Figure 4. The shape and size of the synthesized AgNPs varied depending on the irradiation hours. As the irradiation hours increased, the AgNPs became larger and aggregated. The average diameter of the silver particles was at around 10nm to 14nm. Comparing the absorption spectra of several SF reduced silver colloids prepared under same conditions; we found a good reproducibility [11].

These phenomena were observed in aqueous- stabilized AgNPs and were related to the formate ions and the viscosity of the aqueous solutions. If the viscosity of the polymer solution was decreased, the AgNPs could easily come into contact with other Ag molecules, further aggregation occurred, and the size of AgNPs decreased [12]. It has been reported that silk further the reduction of metal nanoparticles which involves tyrosine groups ionized at basic pH [13]. In fact, molecules containing tyrosine shows excellent reducing agents for synthesis and stabilization of metal nanoparticles in alkaline water [14] or water/alcohol solution as a result of electron transfer mechanism from tyrosine phenolic groups, which are ionized at high pH, to the respective metal ion. On the other hand, irrespective of pH values silk fibers were also found to reduce metal nanoparticles. Thus, silver or gold particles were formed on silk fibers at neutral pH when tyrosine residues were nonionized [15].

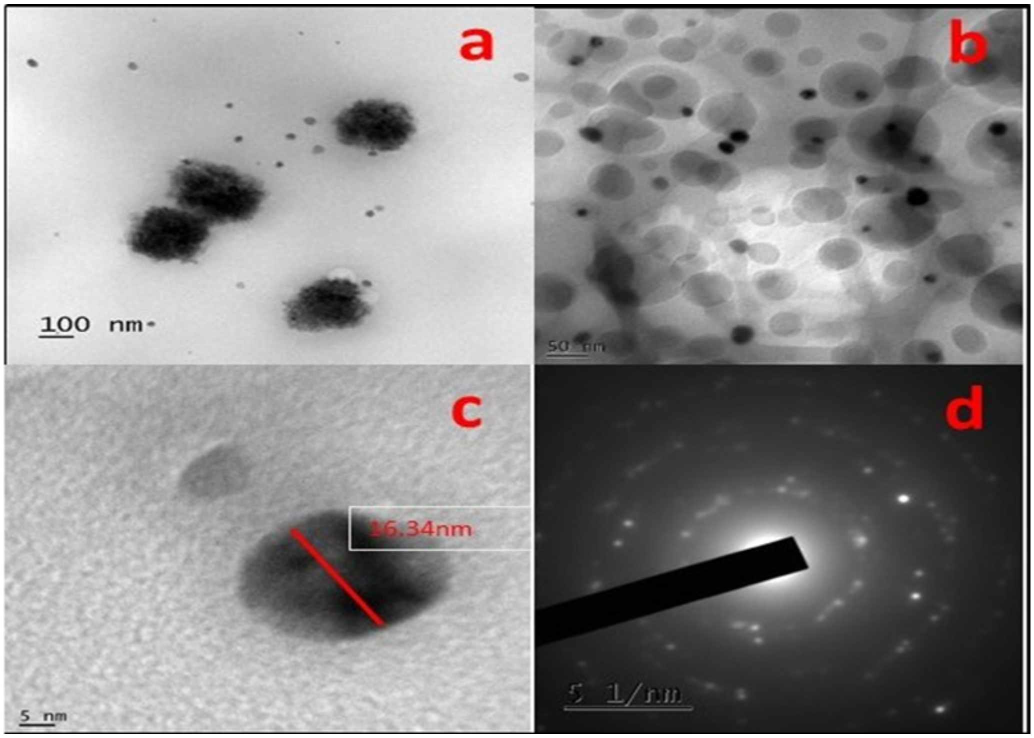


**Fig 4.** (a) TEM images of AgNPs biosynthesized using the Silk fibroin, showing that particles are well dispersed (scale bar: 100 nm), (b) Typical high resolution TEM image of as biosynthesized AgNPs (scale bar: 50 nm), (c) High resolution TEM image of a single AgNPs (scale bar: 5 nm) (d) Typical selected area electron diffraction of AgNPs biosynthesized using Silk fibroin (scale bar: 5 1/nm)

## 3.3 FTIR Analysis

To further explore the in situ synthesis process, FTIR measurements were carried out to identify the possible biochemical radicals among biomolecules, which could be responsible for the reduction of Ag ions to nanoparticles. Figure 5 represents the FTIR spectrum of silver nanoparticles and shows the diagnostic peaks at 1620, 1511, and 1224 $cm^{-1}$. These peaks are assigned to the amide I, amide II, amide III (crystal region, 1224 $cm^{-1}$, amorphous zone, 1260 $cm^{-1}$) bands of proteins released by SFF, respectively, which predominantly indicate $\beta$-sheet structure confirmation, and random coil confirmation.

The peaks at 1620 and 1160 $cm^{-1}$ arise from a carbonyl stretching vibration and phenolic groups of Tyr, which shows the carbonyl stretching vibration from the carboxylate ions and the hydroxyl stretching vibration from the phenolic ions in Tyr of the SF respectively. The carbonyl stretching peak at 1745 $cm^{-1}$ could be assigned to formation of a quinone structure due to oxidation of the phenolic group in Tyr[16]. It has been reported that proteins can bind to metal nanoparticles through either free amine groups or cytosine residues in the proteins. In these circumstances, oxidized tyrosine molecules bounded Ag crystallites through amine groups so that Ag nanoparticles could stabilize, and this is also supported by the shift of the characteristic peaks.

## 3.4 DSC Analysis

The thermal behavior of SF/AgNPs was investigated by means of DSC measurements. The DSC curves displayed two broad endotherms, one at low temperature, due to loss of moisture, another at high temperature (endotherm peak at 294°C), attributed to thermal decomposition of silk[17]. In the 100-200°C temperature range pure silk from silver nanoparticles showed a thermal stability. The decomposition behavior of the silk is influenced by the sample, the degree of molecular orientation being one of the most important parameters[18]. The endothermic peak observed at 370°C in the DSC measurements could be an indication of the formation of stable structure of silver nanoparticles (Figure 6).

Unoriented silk solution with $\beta$-sheet crystalline structure, such as decompose in the 290-295°C temperature range, while decomposition of amorphous silk fibroin occurs at lower temperature (< 290° C).

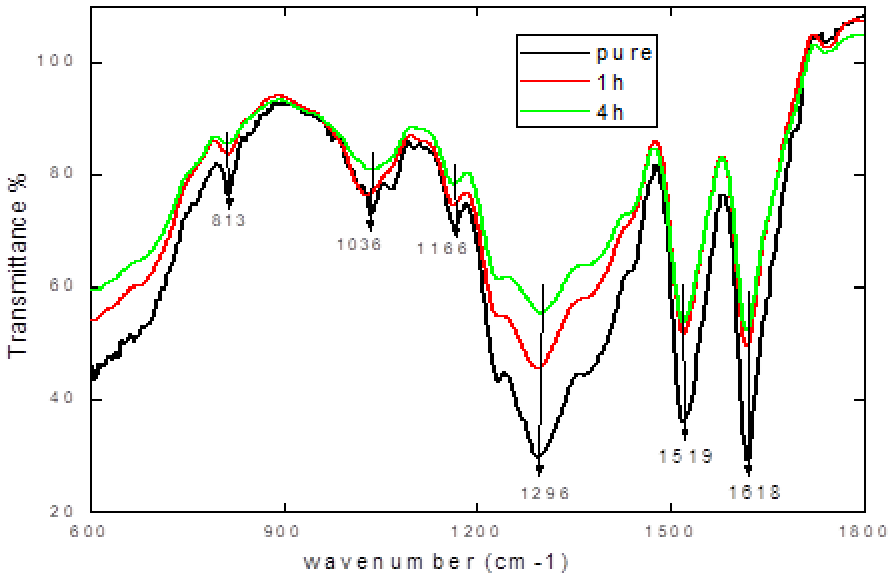


**Fig 5.** FTIR curves of pure SF and SF/AgNPs

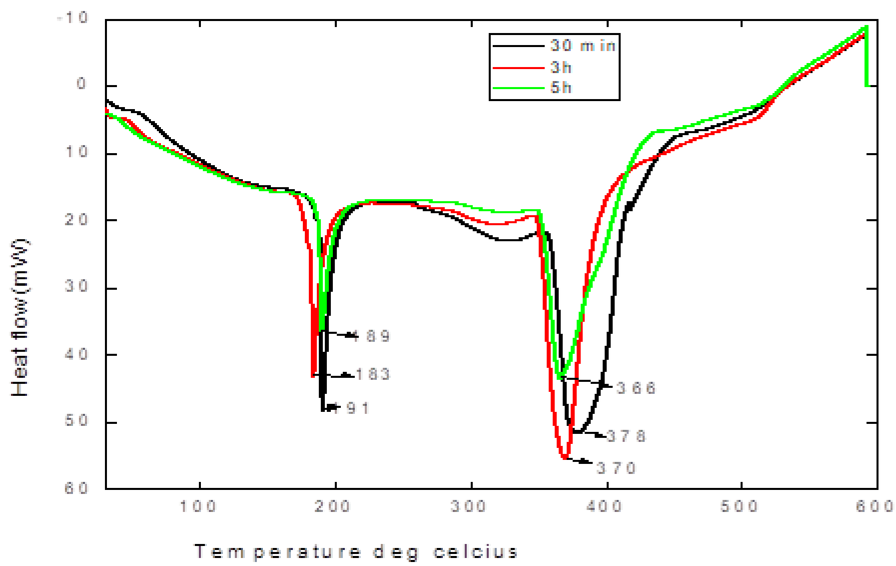


**Fig 6.** DSC graphs of pure SF and SF/AgNPs

## 3.5 TGA Analysis

The thermo gravimetric graphs of SF/AgNPs are shown in Figure 7. The initial weight loss of SF/AgNPs at around 100°C is due to evaporation of moisture. The complete degradation of SF/AgNPs occurred in second stage loss took place within the temperature range between 300°C to 350°C and is associated with the breakdown of the side chain groups of amino acid residues as well as cleavage of peptide bonds[19]. The degradation of SF/AgNPs revealed that the nanocomposites having more stability.

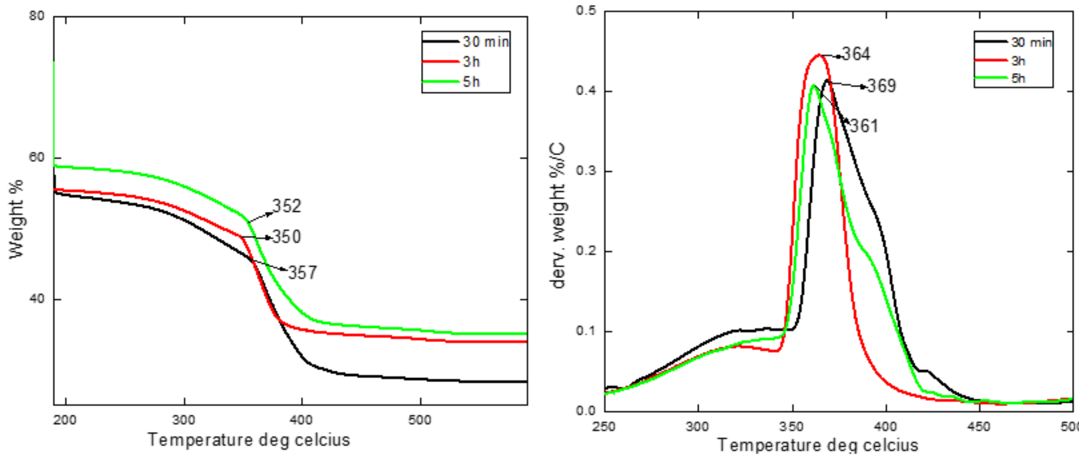


**Fig 7.** (a) TGA graphs of SF/AgNPs and (b) DTG graphs of SF/AgNPs

## 4 Conclusion

The study successfully demonstrates the green synthesis of silver nanoparticles (AgNPs) using an aqueous silk solution as a reducing agent under UVB light irradiation. The formation of AgNPs is evidenced by the color change to dark yellow and confirmed through UV-visible spectroscopy, where an increase in irradiation time correlates with higher absorbance peaks. FTIR analysis indicates the degradation of protein molecules during nanoparticle synthesis. XRD results confirm the crystalline nature of the AgNPs with a face-centered cubic (FCC) structure. TEM imaging reveals a well-distributed morphology of the nanoparticles within the silk solution. Additionally, TGA and DSC analyses suggest that the resulting silk fibroin/Ag nanocomposites exhibit enhanced thermal stability. These findings highlight the potential of using silk fibroin for eco-friendly nanoparticle synthesis with improved material properties.

## References

1) Remita H, Lampre I. Synthesis of Metallic Nanostructures Using Ionizing Radiation and Their Applications. *Materials*. 2024;17:2–364. https://doi.org/10.3390/ma17020364.
2) Dhaka A, Mali SC, Sharma S, Trivedi R. A review on biological synthesis of silver nanoparticles and their potential applications. *Results in Chemistry*. 2023;6:101108. https://doi.org/10.1016/j.rechem.2023.1011083.
3) Alwhibi M, Soliman D, Awad M, Alangery A, Dehaish HA, Alwasel Y. Green synthesis of silver nanoparticles: Characterization and its potential biomedical applications. *Green Processing and Synthesis*. 2021;10(1):412–420. https://doi.org/10.1515/gps-2021-0039.
4) Čubová K, Čuba V. Synthesis of inorganic nanoparticles by ionizing radiation – a review. *Radiation Physics and Chemistry*. 2020;169:108774. https://doi.org/10.1016/j.radphyschem.2020.108774.
5) Naganthran A, Verasoundarapandian G, Khalid FE, Masarudin MJ, Zulkharnain A, Nawawi NM, et al. Synthesis, Characterization and Biomedical Application of Silver Nanoparticles. *Materials*. 2022;15(2):427. https://doi.org/10.3390/ma15020427.
6) Remita H, Lampre I. Synthesis of Metallic Nanostructures Using Ionizing Radiation and Their Applications. *Materials*. 2024;17(2):364. https://doi.org/10.3390/ma17020364.
7) Dhaka A, Mali SC, Sharma S, Trivedi R. A review on biological synthesis of silver nanoparticles and their potential applications. *Results in Chemistry*. 2023;6:101108. https://doi.org/10.1016/j.rechem.2023.101108.
8) Tomii K. Protein Properties. *Encyclopedia of Bioinformatics and Computational Biology*. 2019. Available from: https://www.sciencedirect.com/topics/medicine-and-dentistry/amino-acid-composition.
9) Alzoubi FY, Ahmad AA, Aljarrah IA. Localize surface plasmon resonance of silver nanoparticles using Mie theory. *J Mater Sci: Mater Electron*. 2023;34:2128. https://doi.org/10.1007/s10854-023-11304-x.
10) Shivananda CS. Silk fibroin-based green colloidal silver nanoparticle synthesis and their antibacterial and anticancer properties. *Inorganic Chemistry Communications*. 2023;158:111611. https://doi.org/10.1016/j.inoche.2023.111611.
11) Li A, Chen X, Yao P, Zhang J, Xing T, Chen G. Comparison study on dye degradation by PDA-SF/AgNPs-H2O2 and PDA-SF/AgNPs-PMS catalytic system. *Arabian Journal of Chemistry*. 2023;16(10):105167. https://doi.org/10.1016/j.arabjc.2023.105167.
12) Nie P, Zhao Y, Xu H. Synthesis, applications, toxicity and toxicity mechanisms of silver nanoparticles: A review. *Ecotoxicology and Environmental Safety*. 2023;253:114636. https://doi.org/10.1016/j.ecoenv.2023.114636.
13) Wen Q, Zhang L, Chen Y, Su Y, Yu J, Chen P, et al. Novel Applications of Silk Proteins Based on Their Interactions with Metal Ions. *Sustainability*. 2023;15(22):16053. https://doi.org/10.3390/su152216053.

14) Saragih D, Arifin D, Rusdiarso B, Suyanta S, Santosa S. Synthesis of Silver Nanoparticles Using Tyrosine as Reductor and Capping Agent. *Key Engineering Materials*. 2020;840:360–367. https://doi.org/10.4028/www.scientific.net/KEM.840.360.
15) Korukonda JR, Korumilli T. Instant Synthesis of Silver Particles on Silk Fibres: Characterization and Antimicrobial Study. *Composites Communications*. 2020;18. https://doi.org/10.1016/j.coco.2020.01.004.
16) Su J, Geng Y, Yao J, Huang Y, Ji J, Chen F, et al. Quinone-mediated non-enzymatic browning in model systems during long-term storage. *Food Chem X*. 2022 11;16:100512. https://doi.org/10.1016/j.fochx.2022.100512.
17) Isopencu G, Deleanu I, Busuioc C, Oprea O, Surdu VA, Bacalum M, et al. Bacterial Cellulose—Carboxymethylcellulose Composite Loaded with Turmeric Extract for Antimicrobial Wound Dressing Applications. *International Journal of Molecular Sciences*. 2023;24(2):1719. https://doi.org/10.3390/ijms24021719.
18) Zhang X, Gong D, Gong Y. Insight into the orientation behavior of thermal-aged and historic silk fabrics by polarized FTIR microspectroscopy. *Journal of Cultural Heritage*. 2019;38. https://doi.org/10.1016/j.culher.2019.02.007.
19) Musaimi OA, Lombardi L, Williams DR, Albericio F. Strategies for Improving Peptide Stability and Delivery. *Pharmaceuticals*. 2022;15(10):1283. https://doi.org/10.3390/ph15101283.